



# Structure and mechanical properties of thick Cr/Cr<sub>2</sub>N/CrN multilayer coating deposited by multi-arc ion plating

Lei SHAN<sup>1,2</sup>, Yong-xin WANG<sup>1</sup>, Jin-long LI<sup>1</sup>, He LI<sup>1</sup>, Xia LU<sup>1</sup>, Jian-min CHEN<sup>1</sup>

1. Key Laboratory of Marine Materials and Related Technologies, Zhejiang Key Laboratory of Marine Materials and Protective Technologies, Ningbo Institute of Materials Technology and Engineering, Chinese Academy of Sciences, Ningbo 315201, China
2. Mechanical and Electrical Engineering School, Zhejiang Fashion Institute of Technology, Ningbo 315201, China

Received 25 May 2014; accepted 30 September 2014

**Abstract:** A Cr/Cr<sub>2</sub>N/CrN multilayer coating with a thickness of 24.4 μm was deposited by multi-arc ion plating. The coating was systematically characterized by field emission scanning electron microscopy (FESEM), X-ray photoelectron spectrometry (XPS), energy dispersive spectroscopy (EDS), X-ray diffraction (XRD) and transmission electron microscopy (TEM). Hardness and adhesion were tested by nanoindentation and scratch tester, respectively. The friction properties were investigated by a reciprocating UMT–3MT ball-on-disk tribometer in air and seawater. The results showed that the multilayer coating consisted of three different layers, with Cr, Cr<sub>2</sub>N and CrN phases, respectively. Compared with CrN single layer coating, the adhesion of the multilayer coating was improved significantly, the hardness of the multilayer coating was (21±2) GPa. The corrosion resistance of the multilayer coating was also improved in artificial seawater. The friction coefficient of multilayer coating was lower than that of CrN single layer coating both in air and seawater.

**Key words:** Cr/Cr<sub>2</sub>N/CrN multilayer coating; microstructure; mechanical properties; corrosion resistance; friction

## 1 Introduction

CrN coating is one of the widely used coatings in cutting tools, die and mould, mechanical components and artificial joints to increase their service life due to its excellent oxidation resistance, corrosion resistance, low friction coefficient and high wear resistance [1–7]. Nowadays, great attention has been paid to nano-structured coatings [8,9]. The reason is that the coating should be resistant to abrasive wear, but it also needs to be strain tolerant and tough in order to prevent crack propagation, and therefore avoid fracture or delamination of the coating [10]. In consequence, multilayer coatings were designed to improve wear resistance. It has been reported that nanometric CrN/Cr multilayer coatings have better performance than CrN single layer coatings in abrasion and sliding wear tests [11] and the hardness of CrN/CN<sub>x</sub> multilayer coatings was much higher than that of CrN or CN<sub>x</sub> single layer coatings [12]. Moreover, Cr/CrN coating shows excellent corrosion resistance in

1 mol/L H<sub>2</sub>SO<sub>4</sub> solution [13]. The hardness of Cr<sub>2</sub>N coatings was higher than that of CrN coatings [4], and the Cr<sub>2</sub>N/CrN multilayer coatings improved the wear resistance of the wood machining tools significantly [14,15].

However, there is a lack work on thick Cr/Cr<sub>2</sub>N/CrN multilayer coatings. In this work, Cr<sub>2</sub>N phase with high hardness was introduced into Cr/CrN system to improve the mechanical properties of traditional CrN coatings. In order to obtain the thick Cr/Cr<sub>2</sub>N/CrN coating, alternative deposition of soft Cr layer and hard Cr<sub>x</sub>N layers was applied by multi-arc ion plating. The phase, microstructure and mechanical properties of the coatings were investigated. Comparative experiments of friction behaviors of the multilayer and single layer coatings were carried out in air and seawater.

## 2 Experimental

### 2.1 Coating deposition

As the substrates, the 316L stainless steel

(30 mm × 20 mm × 2 mm) and silicon sheet (30 mm × 10 mm × 0.6 mm) samples were polished to a surface roughness ( $R_a$ ) of 50 nm and ultrasonically cleaned in acetone and ethanol, respectively. The Cr/Cr<sub>2</sub>N/CrN multilayer coating was prepared by a multi-arc ion plating system (Hauzer Flexicoat 850). The substrates were mounted on the holders at 10 cm in front of the targets and applied with a negative bias during deposition. Prior to deposition, the chamber was pumped down to a base pressure below  $4 \times 10^{-3}$  Pa. To remove the thin oxide layer and other adherent impurities, the substrates were etched by Ar<sup>+</sup> bombardments for 2 min with a substrate bias voltage of -900 V. Then, a voltage of -1100 V was applied for 2 min, and followed by a voltage of -1200 V for 2 min as well, to etch the substrates. During coating deposition, the Cr layer was firstly deposited at Ar (99.99%, volume fraction) flow rate of 350 mL/min for 10 min, and then the Cr<sub>2</sub>N layer was deposited in N<sub>2</sub> (99.99%, volume fraction) and Ar mixed atmosphere with flow rates of 50 and 300 mL/min for 10 min, respectively. After that, the flow rate of N<sub>2</sub> increased to 200 mL/min and Ar decreased to 150 mL/min for 10 min, to develop the CrN layer. Three deposition steps of Cr, Cr<sub>2</sub>N and CrN layers were setup as one block. The block was repeated 36 times to form multilayer coating. The rotation speed of the substrate table was 3 r/min, a bias voltage of -25 V and a target current of 65 A were applied during the deposition at 430 °C. Three chromium targets (purity >99.5%,  $d_{63}$  mm × 32 mm) were sputtered. For comparison, CrN single layer coatings were also prepared at N<sub>2</sub> flow rate of 200 mL/min and Ar flow rate of 150 mL/min. The deposition lasted for 18 h. Other deposition parameters were just the same as that of the multilayer coating. All coatings were simultaneously deposited in the same coating batch on silicon, which was used for coating characterization. The coatings deposited on 316L steel were used for mechanical properties tests and tribological tests.

## 2.2 Characterization

The phase structure of the as-deposited coating was investigated by X-ray diffraction (Bruker D8 X-ray facility) using Cu K $\alpha$  radiation ( $\lambda=0.154$  nm), which was operated at 40 kV and 40 mA. The surface morphology and cross-sectional image of the coating were observed by field emission scanning electron microscope (FE-SEM, FEI Quanta FEG 250) equipped with EDS (OXFORD X-Max). The surface roughness ( $R_a$ ) of the coatings was investigated by Alpha-Step IQ profilometer. The elemental compositions were determined by XPS peak area ratios. To verify different layers of the coating, the samples were etched for 5, 25 and 45 min before scanning, respectively. The TEM specimens were

prepared by mechanical grinding and polishing. The crystallinity in different positions along the growth direction of multilayer was verified by selected area electron diffraction (FEI Tecnai G<sup>2</sup> F20 ST). The stress of samples was tested by a residual stress tester (JLCST022 TECH Corp).

The scratching response of the as-deposited coating was evaluated using the CSM Instruments Revetest with a conical diamond tip of 0.2 mm radius and 120° taper angle. During scratch testing the acoustic emission (AE) signals were continuously recorded. Nanoindentation test was carried out by an MTS Nano Indenter@G200 system fitted with a Berkovich indenter using the continuous stiffness measurement (CSM) mode. The corrosion behavior of as-deposited coatings was evaluated by polarization tests (Modulab, Solartron Analytical) in seawater. The seawater was prepared according to Standard ASTM D 1141–98. The chemical composition of artificial seawater was listed in Table 1.

**Table 1** Chemical composition of artificial seawater (g/L)

NaCl	Na <sub>2</sub> SO <sub>4</sub>	MgCl <sub>2</sub>	CaCl <sub>2</sub>	SrCl <sub>2</sub>
24.53	4.09	5.20	1.16	0.025
KCl	NaHCO <sub>3</sub>	KBr	H <sub>3</sub> BO <sub>3</sub>	NaF
0.695	0.201	0.101	0.027	0.003

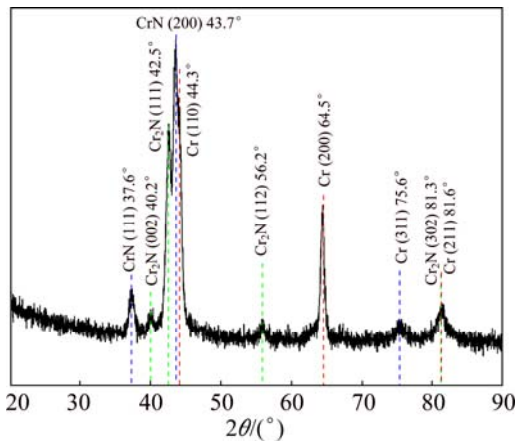
## 2.3 Friction test

Friction tests were performed on a reciprocating ball-on-disk tribometer (CETR UMT-3MT, USA), in sliding contact with WC balls in air and artificial seawater. The WC balls were used as the counterparts with a diameter of 3 mm. A stroke frequency of 5 Hz, a constant normal load of 5 N and a sliding stroke of 5 mm were used in the experiments, and the friction coefficient was continuously recorded during testing. Three samples of each coating were applied for the test. The wear track depth was detected by Alpha-Step IQ profilometer.

## 3 Results and discussion

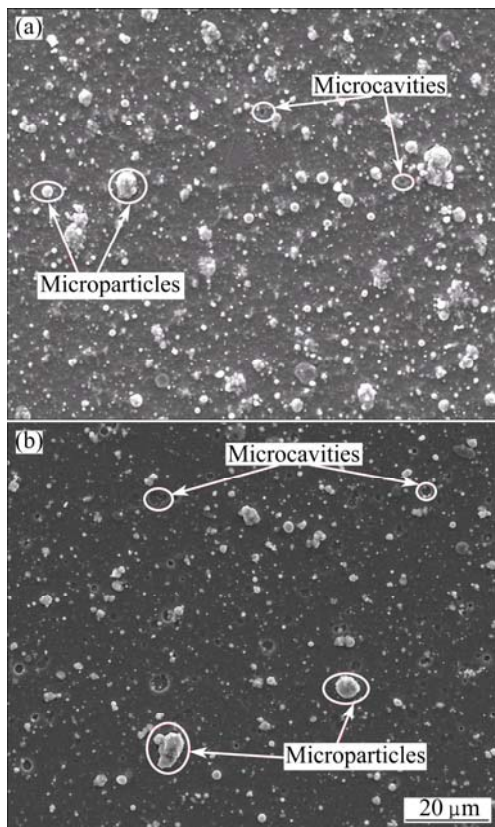
### 3.1 Phase and microstructure of coating

Figure 1 shows the XRD pattern of Cr/Cr<sub>2</sub>N/CrN multilayer coating deposited on 316L stainless steel. The strong peaks at 42.5°, 43.7° and 44.3° represent the Cr<sub>2</sub>N (111), CrN (200) and Cr (110), respectively, according to JCPDS cards 35-0803, 76-2494 and 06-0694. The peak corresponding to CrN (200) is higher than other peaks, which may be attributed to CrN layer at the top. The peaks at 37.6°, 40.2°, 56.2°, 64.5°, 75.6°, 81.3° and 81.6° are also observed corresponding to CrN (111), Cr<sub>2</sub>N (002), Cr<sub>2</sub>N (112), Cr (200), CrN (311), Cr<sub>2</sub>N (302) and Cr (211) respectively. The results are also consistent with values reported in the JCPDS cards mentioned above. The results indicate that the coating mainly contains Cr, Cr<sub>2</sub>N and CrN phases.



**Fig. 1** XRD pattern of Cr/Cr<sub>2</sub>N/CrN multilayer coating

Figure 2(a) shows the surface morphology of the multilayer coating deposited on silicon. It is clear that there are many white particles on the surface of coating. The small microparticles with irregular shapes distribute dispersedly on the coating and protrude out of the coating surface. The microparticles are from droplets emitted from the arc spots of the Cr target [16]. Moreover, a few microcavities are also observed and distribute randomly on the surface of coating. There are two factors accounting for the formation of microcavities: 1) the microparticles are peeled off from the surface



**Fig. 2** Surface morphologies of coatings: (a) Multilayer coating; (b) CrN single layer coating

during the ion bombardment; 2) the microparticles shrank due to the rapid heating/cooling during deposition [17]. It is observed that the number of microcavities is less than that in the single layer coating (Fig. 2(b)), which can be attributed to lower residual stress of the multilayer coating ((0.134±0.005) GPa) than that of single layer coating ((0.461±0.056) GPa). The lower residual stress induces more microparticles adhering to the coating after the deposition. Therefore, the surface roughness (*R<sub>a</sub>*) for the multilayer coating ((150±30) nm) is greater than that of single layer coating ((100±20) nm).

Figure 3(a) shows the fractured cross-sectional morphology of the coating deposited on silicon samples. No signs of delamination between coating and substrate

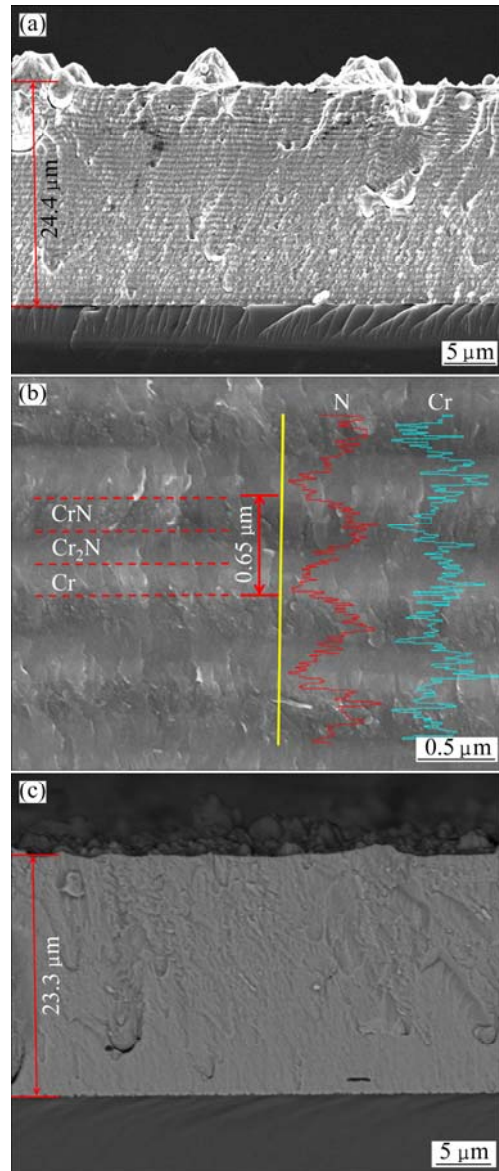


**Fig. 3** Fractured cross-sectional morphology of multilayer coating (a), EDS line scan results of multilayer coating (b) and fractured cross-sectional morphology of CrN single layer coating (c)

or between layers are observed. The interface between layers is relatively flat and clear. The total thickness of the coating is about 24.4  $\mu\text{m}$ , which is thicker than that of a regular coating by PVD methods. However, it is observed that the microparticles also exist inside the coating. In Fig. 3(b), the bright, light grey and dark layers alternating in growth direction are observed because of the difference in the scattering factors of Cr and N. The modulation period of multilayer measured from the image is about 0.65  $\mu\text{m}$  and the thickness of each layer is almost the same. In fact, interfaces between layers are flat and dense without any visible grain boundary porosity. The bright and grey layers present nanocrystal structure and the dark layer presents slight columnar structure. The line scan taken along a marked line is given in Fig. 3(b). The EDS line scan results show the highest content of Cr in the bright layer and the lowest content in the dark layer. The N content presents the opposite profile with the lowest content in bright layer and the highest content in dark layer. This indicates that the change from Cr to CrN phase occurs. The contents of Cr and N fluctuate periodically because of the alternative deposition of Cr, Cr<sub>2</sub>N and CrN layers. As can be seen from Fig. 3(c), the thickness of the CrN single layer coating is about 23.3  $\mu\text{m}$ .

To confirm the composition and valence state of the multilayer coating in different layers, the XPS spectra of Cr 2p<sub>3/2</sub> and N 1s were investigated, as shown in Fig. 4. The Cr 2p<sub>3/2</sub> binding energies for Cr and CrN are 574 eV [18] and 574.5 eV [19], respectively. The N 1s peaks at 397.4 eV are attributed to Cr<sub>2</sub>N, and the peaks at 396.8 eV are related to CrN [20]. In Fig. 4(a), the Cr 2p<sub>3/2</sub> peaks shift to the high binding energy side, and the N 1s peaks shift to the low binding energy side with the increase of etching time (Fig. 4(b)). This indicates that the top layer consists of CrN phase, and with the increase of etching depth, the Cr<sub>2</sub>N and Cr phase are revealed. Thus, the formation of Cr, Cr<sub>2</sub>N and CrN detected by XPS is in good agreement with the EDS line scan results.

Figure 5 shows a bright field TEM image of cross-sectional coating and selected area electron diffraction (SAED) patterns along the growth direction. It is clear that the three layers alternating in growth direction are shown as different colors. The ring pattern in bright area is further identified as Cr (110) and (200), that in the grey area corresponds Cr<sub>2</sub>N (110), (111), (112), (302), and that in the dark area corresponds CrN (111), (200) and (311). The TEM results well match with the XRD results of the coating. In the SAED patterns, the phases along growth direction show the order of Cr, Cr<sub>2</sub>N and CrN. Therefore, the coating consists of three kinds of layers: Cr layer, Cr<sub>2</sub>N layer and CrN layer.

### 3.2 Mechanical properties

Figure 6(a) shows a typical acoustic emission-load graph and track morphology of the multilayer coating. In Fig. 6(a), the curve of acoustic emission is smooth and steady when the normal load is less than 40 N. When the load increases to about 55 N, severe fluctuation of the acoustic signal occurs. Combining with SEM micrographs of scratch tracks in Fig. 6(b), the first crack occurs at the normal load of 63.5 N (LC1). After LC1, intensive cracks occur to form broken coating fractions inside the track and the delamination of the upper coating can be seen at the edge of scratch track. At the end of scratch track in Fig. 6(c), the upper coating is intensively delaminated at the edge of track, and a lot of cracks are also observed inside the scratch track. However, the coating is not totally delaminated from the substrate according to the EDS analysis, which shows that the Fe content is about 30% (mole fraction) and Cr content is over 40% (mole fraction). This indicates that the coating has excellent adhesion to 316L steel substrates. Compared with the adhesion of CrN single layer coating (Fig. 6(d), LC1 value about 39 N), this thick multilayer structure improves the adhesion significantly. A higher critical load for the Cr/Cr<sub>2</sub>N/CrN multilayer coating can be connected with breaking of the columnar growth of

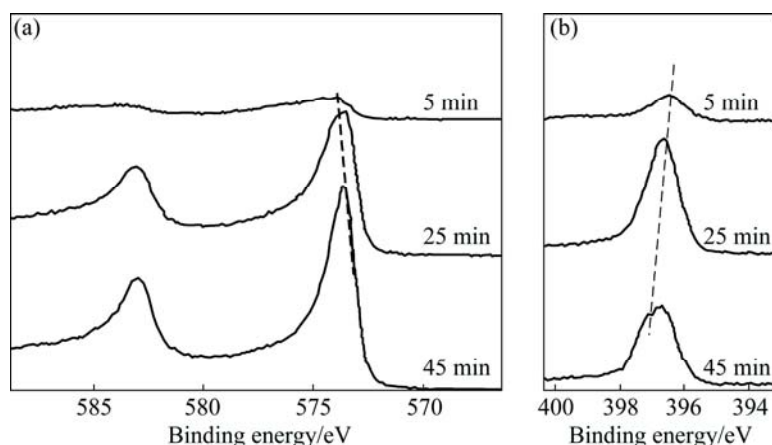
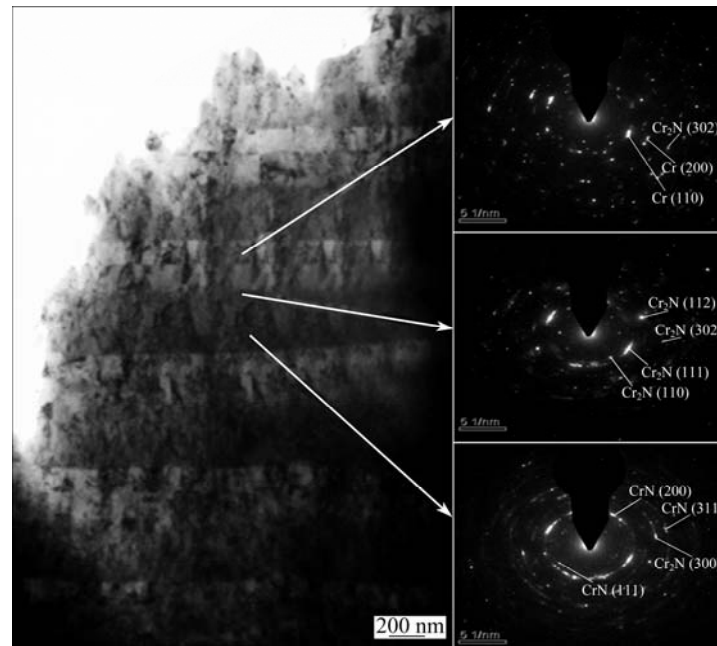
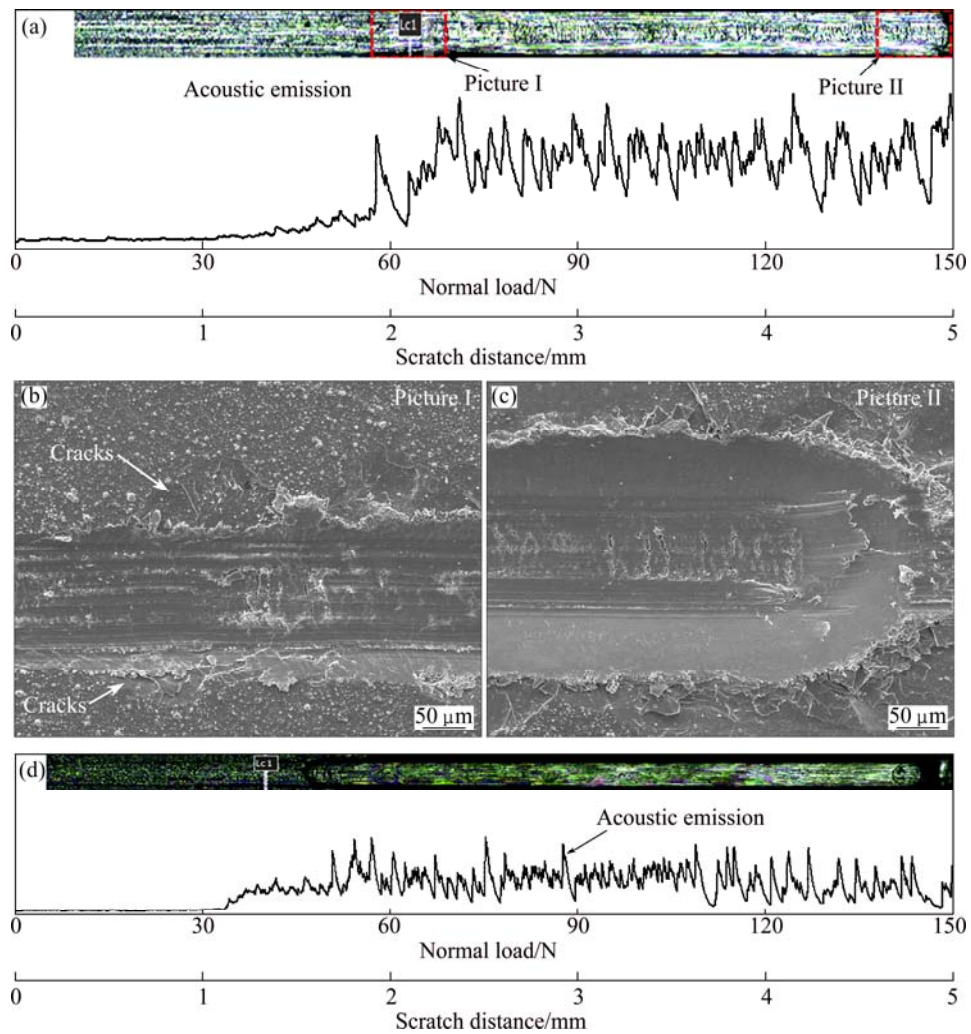


Fig. 4 XPS spectra for multilayer coating: (a) Cr 2p; (b) N 1s



**Fig. 5** TEM image of cross-sectional coating and its SAED patterns at different positions



**Fig. 6** Indenter track and scratch test results of multilayer and single layer coating: (a) Acoustic emission-load graph of multilayer coating; (b) SEM micrograph of scratch tracks of multilayer coating where first crack occurred; (c) Surface morphology at end of scratch track of multilayer coating; (d) Acoustic emission-load graph of single layer coating

the layer and the limitation of the crack propagation only to the layer. It may also be attributed to the lower interfacial stresses for the multilayer coating [21].

Figure 7 shows the hardness of Cr/Cr<sub>2</sub>N/CrN multilayer and CrN single layer coatings with the maximum indentation depth of 1.2 μm. For the thick coatings, no significant contribution to the hardness from substrate is observed with the increase of indentation depth, because the maximum indentation depth is less than 10% of total thickness. The hardness of the single layer coating is (24±3) GPa. The hardness for the multilayer coating is (21±2) GPa according to the platform of the curve. The hardness for the multilayer coating is lower than that of the single layer coating, which can be attributed to the incorporation of soft Cr layer in multilayer coating. However, the hardness of the multilayer coating is slightly higher than that predicted by the rule of mixtures for Cr, Cr<sub>2</sub>N and CrN (about 10 GPa for Cr phase [22], 27.5 GPa for Cr<sub>2</sub>N phase [23] and 24 GPa for CrN phase), which is about 20.5 GPa [24]. The increase of the hardness might be attributed to the presence of interfaces which block the dislocation movement [25].

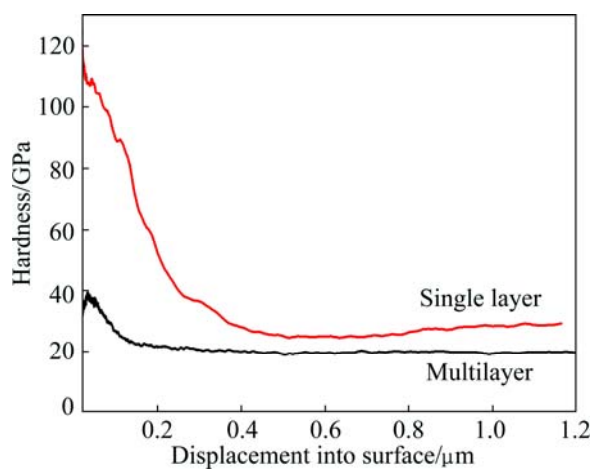


Fig. 7 Hardness of Cr/Cr<sub>2</sub>N/CrN multilayer and CrN single layer coatings with maximum indentation depth of 1.2 μm

### 3.3 Corrosion properties

In order to evaluate the corrosion behavior of the coatings in seawater, the polarization tests were carried out. As shown in Fig. 8, it is clear that the multilayer coating decreases the anodic current density as compared with the single layer coating. The ceramic coatings are chemically inert in neutral media. Therefore, ceramic coatings can separate the substrate from the aggressive environment and protect the substrate if the ceramic coatings are free of defects such as cracks and pinholes. However, the formation of these defects in ceramic coatings is almost impossible to avoid totally. Thus, the coating with denser structure and less defects perform

better in corrosion environment. The multilayer structure can break the columnar growth of the layer and limit the crack propagation only to the layer. Therefore, the multilayer coating reduces the pathways to the substrate and presents better corrosion resistance in seawater.

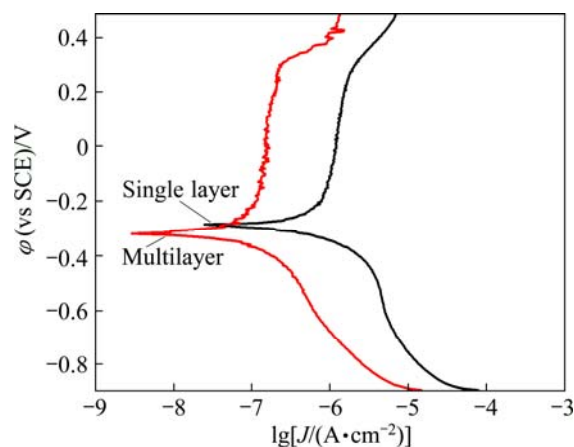


Fig. 8 Polarization curves of multilayer and single layer coatings in seawater

### 3.4 Friction properties

Figure 9 shows the friction behaviors of Cr/Cr<sub>2</sub>N/CrN multilayer and CrN single layer coatings deposited on 316L steel substrates sliding against WC balls in air and seawater. When sliding in air (Fig. 9(a)), the friction coefficient for the multilayer coatings is relatively high at first, and then decreases to the lowest value. The high value is attributed to the rough surface of the coatings and the decrease of friction coefficient represents the run-in period which is caused by rapid increase of the wear of the ball and the coating, which induces smooth sliding interface. After the run-in period, the friction coefficient of the multilayer coating increases. The average friction coefficients for the multilayer coating and single layer coating sliding in air are 0.30±0.03 and 0.44±0.02, respectively. As mentioned before, the multilayer structure can prevent crack propagation and formation of flake pits, therefore making the sliding smoother. To better illustrate friction behavior of the multilayer coating, the wear track profile is introduced, as seen in Fig. 10(a). The first high value of friction coefficient for multilayer coating is due to the rough surface, the relatively low value represents the counter ball sliding against the CrN layer. However, the friction coefficient increases with the increase of the depth of wear track, indicating that the ball mainly slides against the Cr<sub>2</sub>N layer. This is because the friction coefficient of Cr<sub>2</sub>N phase is usually higher than that of CrN phase [20]. The friction coefficient of Cr phase is higher than that of CrN and Cr<sub>2</sub>N phases according to Ref. [26]. Thus, the friction coefficient of the multilayer

coating possesses similar trend in the subsequent sections: gradually increases in one period, which is due to the alternative deposition of Cr, Cr<sub>2</sub>N and CrN layers. However, the difference is not so large which may be attributed to the contact between ball and three layers simultaneously.

values are much lower than those in air, which can be attributed to adsorbed water molecules that may provide boundary lubrication to a certain degree [28]. Thus, the multilayer structure can decrease the friction coefficient both in air and seawater, compared with the single layer coating.

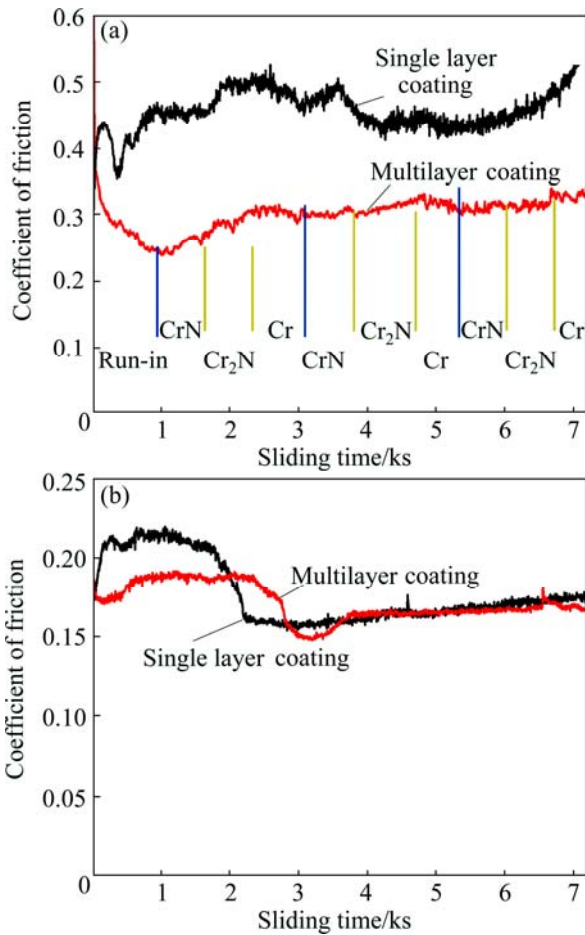


**Fig. 9** Friction behavior of multilayer and CrN single layer coatings sliding against WC balls in air (a) and seawater (b)

When sliding in seawater (Fig. 9(b)), the friction coefficient for the single layer coating firstly increases rapidly, after reaching the highest value, it decreases to the relative steady-state wear stage. The decrease period arises from rapid increase of the wear of ball and coating, which causes that the interface between tribo-pair becomes smoother. Moreover, the continuous removal of tribo-pair by sliding creates extremely smooth surfaces and the upon water condensation from the ambient provides hydrodynamic lubrication [27]. However, no obvious run-in period and no cycle trend are observed in Fig. 9(b) for the multilayer coating. From Fig. 10(b), the maximum wear depth is lower than a period thickness (0.65 μm). The average friction coefficients of the multilayer coating and single layer coating sliding in seawater are 0.17±0.01 and 0.18±0.01, respectively. The

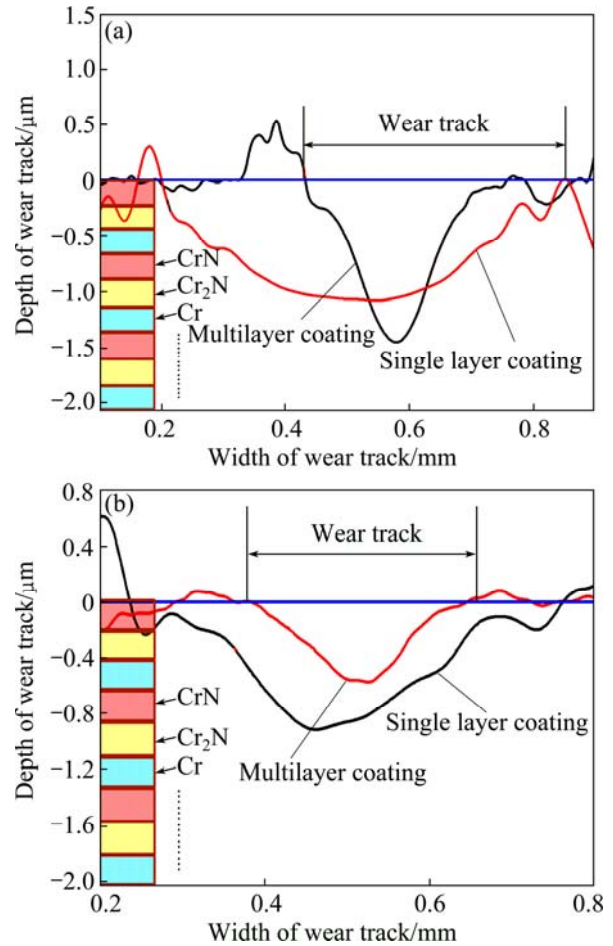


**Fig. 10** Wear track profiles of coatings sliding in air (a) and seawater (b)

### 4 Conclusions

- 1) The Cr/Cr<sub>2</sub>N/CrN multilayer coating with a thickness of 24.4 μm was deposited by multi-arc ion plating. The structure and mechanical properties for the coating were investigated.
- 2) The coating has a dense and compact structure with Cr, Cr<sub>2</sub>N and CrN layers alternating in growth direction.
- 3) The adhesion between coating and substrate is improved by multilayer structure compared with the single layer coating and the hardness for the coating is (21±2) GPa.
- 4) The multilayer coating decreases the anodic current density as compared with the single layer coating. Thus, the corrosion resistance is improved by

the multilayer structure.

5) The friction coefficients of multilayer coating are lower than those of CrN single layer coating both in air and seawater.

## References

- [1] KIM G S, LEE S Y, HAHN J H. Synthesis of CrN/AlN superlattice coatings using closed-field unbalanced magnetron sputtering process [J]. *Surf Coat Technol*, 2003, 171: 91–95.
- [2] CHANG Y Y, WANG D Y. Corrosion behavior of CrN coatings enhanced by niobium ion implantation [J]. *Surf Coat Technol*, 2004, 188: 478–483.
- [3] CHENG Y H, BROWNE T, HECKERMAN B. Mechanical and tribological properties of CrN coatings deposited by large area filtered cathodic arc [J]. *Wear*, 2011, 271: 775–782.
- [4] HONES P, SANJINES R, LEVY F. Characterization of sputter-deposited chromium nitride thin films for hard coatings [J]. *Surf Coat Technol*, 1997, 94–95: 398–402.
- [5] EHIASARIAN A P, HOVSEPIAN P E, HULTMAN L, HELMERSSON U. Comparison of microstructure and mechanical properties of chromium nitride-based coatings deposited by high power impulse magnetron sputtering and by the combined steered cathodic arc/unbalanced magnetron technique [J]. *Thin Solid Films*, 2004, 457: 270–277.
- [6] WANG Q M, KWON S H, KIM K H. Formation of nanocrystalline microstructure in arc ion plated CrN films [J]. *Transactions of Nonferrous Metals Society of China*, 2011, 21(S1): s73–s77.
- [7] LU L, WANG Q M, CHEN B Z, AO Y C, YU D H, WANG C Y, WU S H, KIM K H. Microstructure and cutting performance of CrTiAlN coating for high-speed dry milling [J]. *Transactions of Nonferrous Metals Society of China*, 2014, 24(6): 1800–1806.
- [8] MUSIL J. Hard and superhard nanocomposite coatings [J]. *Surf Coat Technol*, 2000, 125: 322–330.
- [9] WEI Yang-qiong, LI Chun-wei, GONG Chun-zhi, TIAN Xiu-bo, YANG Shi-qin. Microstructure and mechanical properties of TiN/TiAlN multilayer coatings deposited by arc ion plating with separate targets [J]. *Transactions of Nonferrous Metals Society of China*, 2011, 21(5): 1068–1073.
- [10] LUO Q, RAINFORTH W M, MÜNZ W D. TEM observations of wear mechanisms of TiAlCrN and TiAlN/CrN coatings grown by combined steered-arc/unbalanced magnetron deposition [J]. *Wear*, 1999, 225–229: 74–82.
- [11] MARTINEZ E, ROMERO J, LOUSA A, ESTEVE J. Wear behavior of nanometric CrN/Cr multilayers [J]. *Surf Coat Technol*, 2003, 163–164: 571–577.
- [12] VYAS A, SHEN Y G, ZHOU Z F, LI K Y. Nano-structured CrN/CN<sub>x</sub> multilayer films deposited by magnetron sputtering [J]. *Compos Sci Technol*, 2008, 68: 2922–2929.
- [13] NAM N D, KIM M J, JO D S, KIM J G, YOON D H. Corrosion protection of Ti/TiN, Cr/TiN, Ti/CrN, and Cr/CrN multi-coatings in simulated proton exchange membrane fuel cell environment [J]. *Thin Solid Films*, 2013, 545: 380–384.
- [14] WARCHOLINSKI B, GILEWICZ A, RATAJSKI J. Cr<sub>2</sub>N/CrN multilayer coatings for wood machining tools [J]. *Tribol Int*, 2011, 44: 1076–1082.
- [15] FAGA M G, SETTINERI L. Innovative anti-wear coatings on cutting tools for wood machining [J]. *Surf Coat Technol*, 2006, 201: 3002–3007.
- [16] WAN X S, ZHAO S S, YANG Y, GONG J, SUN C. Effects of nitrogen pressure and pulse bias voltage on the properties of Cr–N coatings deposited by arc ion plating [J]. *Surf Coat Technol*, 2010, 204: 1800–1810.
- [17] ZHANG S H, WANG L, WANG Q M, LI M X. A superhard CrAlSiN superlattice coating deposited by multi-arc ion plating: I. Microstructure and mechanical properties [J]. *Surf Coat Technol*, 2013, 214: 160–167.
- [18] CONDE A, CRISTÓBAL A B, FUENTES G, TATE T. Surface analysis of electrochemically stripped CrN coatings [J]. *Surf Coat Technol*, 2006, 201: 3588–3595.
- [19] ZHANG S H, LI M X, HE Y Z, CHO T Y, CHUN H G, YOON J, SI S H, LI H S. Synthesis and properties of CrN<sub>x</sub>/amorphous-WC nanocomposites prepared using hybrid arc ion plating and direct current magnetron sputtering [J]. *Thin Solid Films*, 2010, 519: 751–758.
- [20] KONG Q H, JI L, LI H X, LIU X H, WANG Y J, CHEN J M, ZHOU H D. Composition, microstructure, and properties of CrN<sub>x</sub> films deposited using medium frequency magnetron sputtering [J]. *Appl Surf Sci*, 2011, 257: 2269–2274.
- [21] VOEVODIN A A, IARVE E V, RAGLAND W, ZABINSKI J S, DONALDSON S. Stress analyses and in-situ fracture observation of wear protective multilayer coatings in contact loading [J]. *Surf Coat Technol*, 2001, 148: 38–45.
- [22] ZENG Z X, WANG L P, CHEN L, ZHANG J Y. The correlation between the hardness and tribological behaviour of electroplated chromium coatings sliding against ceramic and steel counterparts [J]. *Surf Coat Technol*, 2006, 201: 2282–2288.
- [23] SHAN L, WANG Y X, LI J L, CHEN J M. Effect of N<sub>2</sub> flow rate on microstructure and mechanical properties of PVD CrN<sub>x</sub> coatings for tribological application in seawater [J]. *Surf Coat Technol*, 2014, 242: 74–82.
- [24] KIM S H, BAIK Y J, KWON D. Analysis of interfacial strengthening from composite hardness of TiN/VN and TiN/NbN multilayer hard coatings [J]. *Surf Coat Technol*, 2004, 187: 47–53.
- [25] KOEHLER J S. Attempt to design a strong solid [J]. *Phys Rev B*, 1970, 2: 547–551.
- [26] LIN J, WU Z L, ZHANG X H, MISHRA B, MOORE J J, SPROUL W D. A comparative study of CrN<sub>x</sub> coatings synthesized by dc and pulsed dc magnetron sputtering [J]. *Thin Solid Films*, 2009, 517: 1887–1894.
- [27] ROOS J R, CELIS J P, VANCOILLE E, VELTROP H, BOELENS S, JUNGBLUT F, EBBERINK J, HOMBERG H. Interrelationship between processing, coating properties and functional properties of steered arc physically vapour deposited (Ti,Al) N and (Ti,Nb) N coatings [J]. *Thin Solid Films*, 1990, 193: 547–556.
- [28] SHAN L, WANG Y X, LI J L, LI H, WU X D, CHEN J M. Tribological behaviours of PVD TiN and TiCN coatings in artificial seawater [J]. *Surf Coat Technol*, 2013, 226: 40–50.

# 多弧离子镀制备的大厚度 Cr/Cr<sub>2</sub>N/CrN 多层涂层的结构和力学性能

单磊<sup>1,2</sup>, 王永欣<sup>1</sup>, 李金龙<sup>1</sup>, 李赫<sup>1</sup>, 鲁侠<sup>1</sup>, 陈建敏<sup>1</sup>

1. 中国科学院 海洋新材料与应用技术重点实验室, 浙江省海洋材料与防护技术重点实验室, 中国科学院 宁波材料技术与工程研究所, 宁波 315201;
2. 浙江纺织服装职业技术学院 机电与轨道交通学院, 宁波 315201

**摘要:** 采用多弧离子镀制备一种厚度为 24.4 μm 的 Cr/Cr<sub>2</sub>N/CrN 多层结构涂层。采用场发射扫描电子显微镜 (FESEM)、X 射线光电子能谱 (XPS)、能量散射谱 (EDS)、X 射线衍射 (XRD) 和透射电镜 (TEM) 对涂层进行表征, 并用纳米压痕和划痕仪测试其硬度和结合力。用 UMT-3MT 往复式摩擦磨损试验机对涂层在大气和海水环境中的摩擦性能进行测试。结果表明, 该涂层由 3 种相结构组成, 分别是 Cr 相、Cr<sub>2</sub>N 相和 CrN 相。相对于单层 CrN 涂层, 多层涂层的结合力明显提高, 该涂层的硬度为 (21±2) GPa。多层结构涂层在人工海水中的耐蚀性能显著优于单层 CrN 涂层的耐蚀性能, 且在大气和海水中多层结构涂层的摩擦因数均低于单层 CrN 涂层的摩擦因数。

**关键词:** Cr/Cr<sub>2</sub>N/CrN 多层涂层; 显微结构; 力学性能; 耐蚀性; 摩擦

(Edited by Wei-ping CHEN)